Flux dependence of cluster formation in neutron-irradiated weld material

2008 J. Phys.: Condens. Matter 20 104262

(http://iopscience.iop.org/0953-8984/20/10/104262)

J. Phys.: Condens. Matter **20** (2008) 104262 (6pp) doi:10.1088/0953-8984/20/10/104262

Flux dependence of cluster formation in neutron-irradiated weld material

F Bergner[1], A Ulbricht[1], H Hein[2] and M Kammel[3]

[1] Forschungszentrum Dresden-Rossendorf, PF 510119, 01314 Dresden, Germany
[2] AREVA NP, Freyeslebenstraße 1, 91058 Erlangen, Germany
[3] Hahn-Meitner-Institut, Glienicker Straße 100, 14109 Berlin, Germany

E-mail: F.Bergner@fzd.de

Received 16 July 2007, in final form 24 September 2007
Published 19 February 2008
Online at stacks.iop.org/JPhysCM/20/104262

Abstract
The effect of neutron flux on the formation of irradiation-induced clusters in reactor pressure vessel (RPV) steels is an unresolved issue. Small-angle neutron scattering was measured for a neutron-irradiated RPV weld material containing 0.22 wt% impurity Cu. The experiment was focused on the influence of neutron flux on the formation of irradiation-induced clusters at fixed fluence. The aim was to separate and tentatively interpret the effect of flux on the characteristics of the cluster size distribution. We have observed a pronounced effect of neutron flux on cluster size, whereas the total volume fraction of irradiation-induced clusters is insensitive to the level of flux. The result is compatible with a rate theory model according to which the range of applied fluxes covers the transition from a flux-independent regime at lower fluxes to a regime of decelerating cluster growth. The results are confronted with measured irradiation-induced changes of mechanical properties. Despite the observed flux effect on cluster size, both yield stress increase and transition temperature shift turned out to be independent of flux. This is in agreement with the volume fraction of irradiation-induced clusters being insensitive to the level of flux.

(Some figures in this article are in colour only in the electronic version)

1. Introduction

The material at a given position of a near-core nuclear reactor component or the material of a sample placed in an irradiation capsule is exposed to a neutron flux, φ, and accumulates, with elapsing exposure time, t, a neutron fluence, $\psi = \varphi t$. While it is straightforward to tackle the issue of the fluence dependence of material properties, in particular those related to embrittlement, by varying the exposure time, it is much more difficult to extract flux effects. In fact, different values of flux have to be compensated for by inversely related exposure times in order to keep the value of the fluence constant. That means that irradiations at a low flux require long exposure times, more than 20 years in some cases, in order to accumulate the required fluence. Furthermore, different values of flux are usually interrelated with differences of both neutron spectrum and irradiation temperatures as well as variations of composition. The authors examined a reactor pressure vessel (RPV) weld material exposed to fluxes differing by a factor of 35, while fluence and irradiation temperature are essentially equal. The irradiation time of the material exposed to the lower flux was as long as 11.6 years.

The issue of flux dependence is important for several reasons, the first of which is related to the safety assessment procedure based on surveillance specimens and lead factors [1]. These specimens are irradiated at a higher flux (lead factors of 3–5 [1]) than the RPV material to be evaluated, which means the required fluence is accumulated in advance and the future behaviour of the material can be anticipated. The validation of the procedure requires among others a well-founded knowledge on the flux effect. Secondly, with respect to life time extensions for nuclear reactors to 40 years and beyond, considerable levels of neutron fluence may be accumulated at positions exposed to very low fluxes. The complex issue of the transferability of high-flux data to lower fluxes is one of the motivations for the advanced modelling approaches such as mechanistically based correlations (MBC) [2, 3] and multiscale-multiphysics (MSMP) modelling [4–7]. These models, while gaining much insight (and hopefully predictive capabilities in future), require

validation based on experiments performed under well-defined conditions including a broad range of fluxes.

The flux dependence of the microstructure and the mechanical properties of RPV steels and related model alloys is still an unresolved issue [1, 8]. Flux effects also depend on chemical composition. For pure Fe under irradiation, the balance equation for single vacancies combines a generation term, which is proportional to flux, a term describing the recombination of vacancies with self-interstitial atoms (SIA) and a sink term, see (1) and (2) below. The discussion of both the flux dependence of the steady-state vacancy concentration and the vacancy-assisted diffusion of Cu shows that flux independence of the microstructure is expected at lower fluxes and a pronounced dependence of the microstructure on flux is expected at higher fluxes. A number of three effects contributing to flux dependence was identified and described on the basis of rate theory in [8]. Details not amenable to rate theory were recently resolved using kinetic Monte Carlo (KMC) simulations [9]. It was also observed from KMC simulations [10] that jumps of thermally induced vacancies assume an increasing fraction of the total number of jumps per unit of exposure time, when the dose rate decreases. This suggests that the accelerated embrittlement at low flux may be partly caused by thermal ageing effects. Alloys of increasing complexity are currently being investigated in the framework of MSMP modelling.

For RPV steels, increased flux can either increase, decrease or not influence embrittlement, depending on the specific combination of irradiation temperature, flux, fluence and alloy Cu and Ni content [11–13]. Empirical multi-parameter correlation approaches have been applied successfully in order to separate flux effects from such combined effects on irradiation embrittlement or hardening [8, 14–16]. In many studies minor or no flux dependence of embrittlement or hardening was detected. This can either mean that there is no effect, or the covered flux range was too small or significant flux effects on the microstructure exist but are unimportant for the mechanical properties or cancel out each other. Few studies deal with the flux dependence of the microstructure. Flux effects are included in one of the most comprehensive small-angle neutron scattering (SANS) investigations of RPV steels [17], but these are always mixed with the effect of fluence. Odette [8] notes that the results of a study on the flux dependence of irradiation hardening are generally consistent with a similar analysis of SANS data, but the SANS study seems to be still unpublished.

In this paper, SANS was applied to investigate the size distribution of irradiation-induced solute clusters in an RPV weld material of a relatively high level of impurity Cu (0.22 wt%). While the material was exposed to neutron irradiations at two different levels of neutron flux, the same value of neutron fluence was accumulated in both cases in order to separate the flux effect. The observed microstructures are confronted with the resulting irradiation-induced changes of mechanical properties. Results for a similar low-Cu weld material are included, in order to check the assumption on the dominant role of Cu. Furthermore, the behaviour observed for the high-Cu weld is contrasted with earlier results for another RPV steel exhibiting the opposite behaviour.

Table 1. Composition of investigated materials (wt%).

	C	Si	P	S	V	Cr	Mn	Ni	Cu	Mo
Weld 1	0.08	0.15	0.015	0.017	0.001	0.74	1.10	1.11	0.22	0.60
Weld 2	0.07	0.15	0.017	0.010	0.011	0.10	1.06	1.00	0.03	0.62

Table 2. Irradiation conditions (fluence and flux values for neutron energy, $E > 1$ MeV).

	Code	Fluence (cm^{-2})	Flux ($cm^{-2}\ s^{-1}$)	Time	Temperature (°C)
Weld 1	I-1	2.2×10^{19}	2.1×10^{12}	122 days	285
Weld 1	I-2	2.2×10^{19}	6.0×10^{10}	11.6 years	288
Weld 2	I-3	1.4×10^{19}	3.6×10^{12}	44.6 days	285

Table 3. Irradiation induced changes of yield stress, σ_y, and brittle–ductile transition temperature, T_{41}. Measuring uncertainties are of the order of 10%.

	Code	$\Delta\sigma_y$ (MPa)	ΔT_{41} (K)
Weld 1	I-1	211	119
Weld 1	I-2	196	111
Weld 2	I-3	61	0

2. Experiments

The material investigated is a first generation submerged weld NiCrMo1 UP (modified)/LW320, LW340 (German specification) containing an impurity Cu level of 0.22 wt%. It is denoted by weld 1 here. A fourth generation submerged weld NiMo1/OP41 TT UP containing 0.03 wt% Cu (weld 2) is included in the investigation for comparison. The compositions are given in table 1, the irradiation conditions are summarized in table 2 and the irradiation-induced mechanical property changes are compiled in table 3. Slices of cross-sectional area of 10 mm × 10 mm and of 1 mm thickness were prepared for the SANS experiment.

The SANS measurements were performed at the instrument V4 of Hahn-Meitner-Institut Berlin [18]. The samples were placed in a magnetic field of 1.2 T perpendicular to the incident neutron beam. The beam diameter was 7.5 mm and the neutron wavelength was 0.6 nm. Two sample-detector distances of 1.1 and 4 m were chosen, thus covering a range of scattering vectors, Q, from 0.2 to 3.0 nm^{-1}. The collimation length of the neutron beam was 2 and 4 m, respectively. The raw-data treatment, including transmission measurement and correction for both background and detector sensitivity, is described in [19]. For absolute calibration the water standard was used. Data analysis including separation of magnetic and nuclear scattering cross-sections was performed using the BerSANS software package [20]. The incoherent scattering cross-sections were determined on the basis of Porod plots and subtracted from the total cross-sections. The unirradiated conditions for each material were taken as reference.

Further analysis is based on the indirect transformation method [21] and provides the size distribution of scatterers without assuming a certain type of distribution. The resolution limits of SANS for the present conditions are 0.5 nm

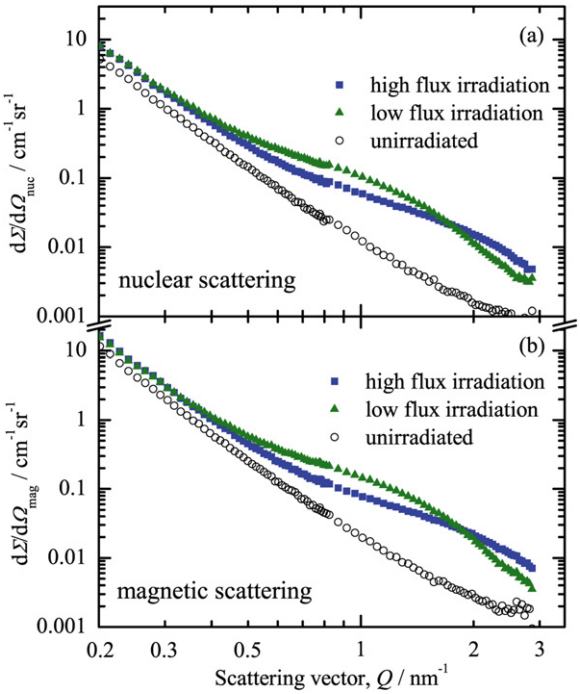

Figure 1. Coherent nuclear (a) and magnetic (b) scattering cross-sections obtained for weld 1 (0.22 wt% Cu).

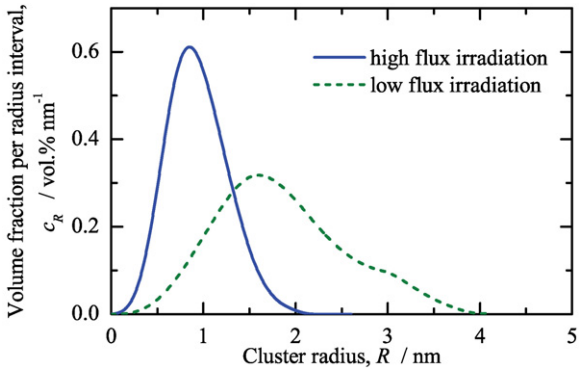

Figure 2. Size distribution of irradiation-induced clusters reconstructed for weld 1.

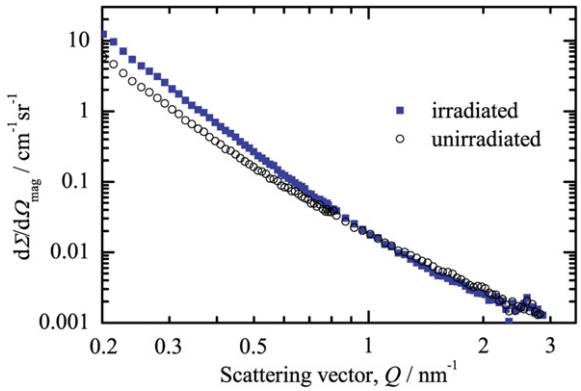

Figure 3. Coherent magnetic scattering cross-section obtained for weld 2 (0.03 wt% Cu).

and 0.005% with respect to the radius and to the total volume fraction of scatterers, respectively. According to our standard analysis we have assumed that the system consists of isolated scattering particles in a homogeneous matrix (two-phase approach) and that the particles are spherical and non-magnetic. The A-ratio, originally defined as the ratio of the scattering cross-sections perpendicular and parallel to the magnetic field direction [22], was calculated in the size space after performing the transformation according to the relation, $A = 1 + M/N$, where M and N denote the area under the size distribution curve obtained from the magnetic and nuclear scattering contributions, respectively.

3. Results and discussion

The coherent magnetic and nuclear scattering cross-sections, $d\Sigma/d\Omega$, obtained for weld 1 and the reconstructed volume-related size distributions are plotted in figures 1 and 2, respectively. The scattering cross-sections of the low-flux and high-flux irradiations exhibit characteristic differences manifesting themselves in different size distributions. The magnetic and nuclear contributions exhibit the same behaviour, that is, the magnetic and nuclear contrasts are caused by the same objects. The coherent magnetic scattering cross-section obtained for the low-Cu weld 2 is presented in figure 3. The scattering curves for the irradiated and unirradiated condition can be considered to be equal within experimental uncertainty especially in the high-Q range, where irradiation-induced effects are expected. It can be concluded that the total volume fraction of irradiation-induced scatterers (if any) is less than 0.005%.

Table 4. Parameters of irradiation-induced clusters detected by SANS.

	Code	Peak radius (nm)	Volume fraction (%)	Number density (cm^{-3})	A-ratio
Weld 1	I-1	0.85	0.51 ± 0.02	17×10^{17}	2.3 ± 0.1
	I-2	1.6	0.53 ± 0.02	5×10^{17}	2.5 ± 0.1
Weld 2	I-3	—	<0.005	—	—

The results of the SANS measurements are summarized in table 4. The increase of the peak radius of the volume-related size distribution of scatterers for weld 1 by a factor of about 2 is the most prominent effect of reducing the flux by a factor of 35 at constant fluence. The total volume fraction of scatterers is approximately independent of flux. The increase of size at constant volume fraction requires the number density to decrease as shown in table 4. A more detailed description of the size distribution can be obtained from figure 2. The maximum size of scatterers detected by SANS increases from 2 nm for the higher flux to 4 nm for the lower flux. The size distribution obtained for the lower flux seems to consist of two overlapping components. However, these cannot be separated without assumptions on the type of distribution.

We have observed that the A-ratio is approximately independent of flux. This is an indication of similar

compositions of the scatterers in both cases. On the one hand, the A-ratio of about 2.4 implies that the scatterers are not pure Cu, which would require a much higher A-ratio [23]. This is confirmed by the measured total volume fractions, which are significantly larger than the volume fraction of pure Cu clusters accessible due to the Cu content of weld 1. On the other hand, the fact that no irradiation-induced scatterers are observed for weld 2 (containing only 0.03 wt% Cu) shows the decisive role of Cu in the formation process of clusters. In fact, atom probe investigations performed for similar RPV materials confirm that Cu is an important constituent of the clusters [24, 25]. These results and the background presented in the introduction indicate that irradiation-enhanced Cu diffusion controlled by the vacancy concentration could be responsible for the observed flux effect. In order to check this possibility, we apply a simplified rate theory approach below.

The rates of change of the vacancy concentration, C_v, and the self-interstitial atom (SIA) concentration, C_i, are described by (1) and (2), respectively [26].

$$\frac{\mathrm{d}C_\mathrm{v}}{\mathrm{d}t} = G_\mathrm{v} - \frac{4\pi r(D_\mathrm{v}+D_\mathrm{i})C_\mathrm{v}C_\mathrm{i}}{\Omega_\mathrm{a}} - K_\mathrm{v}C_\mathrm{v} \qquad (1)$$

$$\frac{\mathrm{d}C_\mathrm{i}}{\mathrm{d}t} = G_\mathrm{i} - \frac{4\pi r(D_\mathrm{v}+D_\mathrm{i})C_\mathrm{v}C_\mathrm{i}}{\Omega_\mathrm{a}} - K_\mathrm{i}C_\mathrm{i} \qquad (2)$$

G_v and G_i are the production rates of free vacancies and free SIA due to neutron irradiation, $K_\mathrm{v} = D_\mathrm{v}S_\mathrm{v}$ and $K_\mathrm{i} = D_\mathrm{i}S_\mathrm{i}$ are the reaction rate constants, D_v and D_i are the diffusivities of vacancies and SIA, S_v and S_i are the sink strengths for vacancies and SIA, respectively. Ω_a is the atomic volume of iron, r is the recombination or trap radius. In the steady state, the left-hand sides of (1) and (2) vanish and the steady-state vacancy concentration, C_vss, can be expressed by solving a quadratic. We shall focus on the flux dependence here:

$$C_\mathrm{vss} = 2.4C_\mathrm{vss,t}\left(\sqrt{1+\frac{\varphi}{\varphi_\mathrm{t}}}-1\right) \qquad (3)$$

φ is the flux and φ_t is the value of the flux at the transition between two regimes of the flux dependence. $C_\mathrm{vss,t}$ is the steady-state vacancy concentration at the flux, $\varphi = \varphi_\mathrm{t}$. The expression in parentheses is asymptotically proportional to φ for $\varphi \ll \varphi_\mathrm{t}$ and to $\varphi^{1/2}$ for $\varphi \gg \varphi_\mathrm{t}$. φ_t is given by [8]:

$$\varphi_\mathrm{t} = \frac{\Omega_\mathrm{a}D_\mathrm{v}S_\mathrm{v}^2}{16\pi r\xi\sigma_\mathrm{dpa}} \qquad (4)$$

σ_dpa is the displacement-per-atom (dpa) cross-section and ξ is the fraction of vacancies and SIA created per dpa. Rate theory of the evolution of Cu clusters [23] shows that cluster growth is governed by the dimensionless parameter $D^*_\mathrm{Cu}t/a^2$, where t is the irradiation time, D^*_Cu is the irradiation-enhanced diffusion coefficient of Cu in Fe and a is the lattice parameter of bcc Fe. We use the approximation [2]:

$$D^*_\mathrm{Cu} = D_\mathrm{Cu}\frac{C_\mathrm{vss}}{C_\mathrm{veq}}. \qquad (5)$$

Here D_Cu and C_veq are Cu diffusivity and vacancy concentration in thermal equilibrium, respectively. Therefore, we arrive at the conclusion that the cluster growth at a given value of fluence, ψ, is a monotonically decreasing function of flux and its behaviour is governed by the kinetics parameter, k, according to:

$$k = D^*_\mathrm{Cu}t/\psi \sim \begin{cases} \text{constant} & \varphi \ll \varphi_\mathrm{t} \\ 1/\sqrt{\varphi} & \varphi \gg \varphi_\mathrm{t}. \end{cases} \qquad (6)$$

An estimation of the transition flux, φ_t, using $S_\mathrm{t} = 10^{14}$ m^{-2} (i.e. the order of magnitude of the dislocation density), D_v (285 °C) $= 10^{-16}$ m^2 s^{-1}, $r = 0.574$ nm, $\xi = 0.4$ and $\sigma_\mathrm{dpa} = 1.5 \times 10^{-25}$ m^2 [8] gives $\varphi_\mathrm{t} = 7 \times 10^{11}$ cm^{-2} s^{-1}. The kinetics parameter, k, normalized with the flux-independent limit, k_0, at low fluxes is plotted in figure 4 as a function of the normalized flux, $\varphi/\varphi_\mathrm{t}$. We expect the lower-flux condition for weld 1 (condition I-2 in table 2) to be in the flux-independent regime of cluster growth and the higher-flux condition (condition I-1 in table 2) to be outside and to exhibit a noticeably slower cluster growth. This is what we have observed according to table 4. As we know that only less than 50% of the cluster volume fraction is occupied by Cu atoms, the above estimation is not suitable for a quantitative prediction of measured cluster size.

In order to show the specificity of the observed cluster growth, we compare the result with an earlier finding for an RPV steel containing 0.15% Cu (table 5) [27–29] exposed

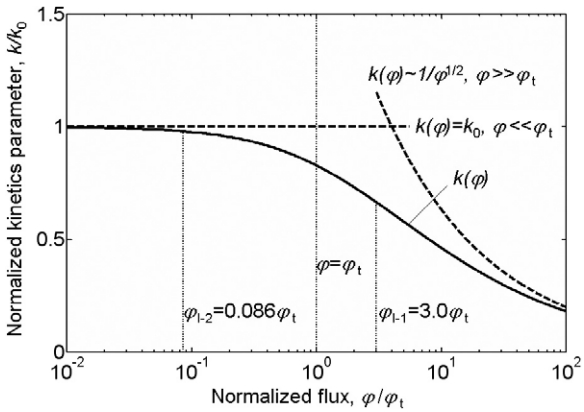

Figure 4. Normalized kinetics parameter, k/k_0, which governs cluster growth, as a function of normalized flux, $\varphi/\varphi_\mathrm{t}$. Solid line: rate theory model according to (3)–(6), dashed lines: asymptotic behaviour according to (6), dotted lines: experimental fluxes according to table 2 expressed in terms of multiples of φ_t according to (4).

Table 5. Irradiation conditions, SANS results and brittle–ductile transition temperature shift for a reference RPV steel containing 0.15 wt% Cu (irradiation temperature 255 °C, fluence and flux values for neutron energy, $E > 1$ MeV).

Fluence (cm^{-2})	Flux (cm^{-2} s^{-1})	Peak radius (nm)	Volume fraction (%)	A-ratio	ΔT_{41} (K)
7.0×10^{18}	1.0×10^{11}	1.0	0.21 ± 0.01	2.1 ± 0.2	125
5.4×10^{19}	2.1×10^{12}	1.0	0.34 ± 0.01	2.4 ± 0.2	178
9.6×10^{19}	3.7×10^{12}	1.0	0.50 ± 0.02	2.6 ± 0.2	221

to neutron irradiations at varying fluence and flux. The pronounced increase of the volume fraction of clusters is clearly an effect of increasing neutron fluence. However, in contrast with the present findings, this steel does not exhibit any detectable differences in cluster size, although wide variations of both fluence and flux were included in the experiment. A possible explanation is the considerably lower irradiation temperature (255 °C versus 285 °C). Differences in composition may also play a role. The comparison also points to the importance to separate fluence and flux effects.

Comparing the flux effects on microstructure with the mechanical properties, we have found that the observed differences of cluster size are not reflected in corresponding differences of irradiation-induced changes of the mechanical properties. In fact, the differences in yield stress increase and transition temperature shift (table 3) are in the range of the experimental uncertainty. This finding is partly in conflict with expectations according to the Russell–Brown model of dispersion strengthening [30]. This model predicts a proportionality of the yield stress increase to the inverse of the planar spacing between the obstacles, L, given by [30]:

$$L^{-1} = \frac{\sqrt{c}}{1.77R} \tag{7}$$

c is the volume fraction of Cu-rich clusters, which are assumed to be the dominant irradiation-induced obstacles for dislocation glide here, and R is the mean planar cluster radius. These results were more recently confirmed by means of molecular dynamics simulations of the interaction of dislocations with Cu clusters in Fe [31]. Although the peak radius calculated in the present investigation is not identical with the mean planar radius, there is clearly a conflict between the observed insensitivity of the yield stress increase to the peak radius (table 3) and the predicted inverse proportionality to R at constant volume fraction, c. As there is strong evidence for a proportionality of yield stress increase and brittle–ductile transition temperature shift [3], the same reasoning also applies to the latter quantity (table 3). On the other hand, the c-dependence according to (7) is consistent with the simultaneous agreement of the volume fractions and mechanical property changes measured for weld 1. The present result is an example where a pronounced flux effect on the mechanical properties is absent, but certain microstructural features do depend on flux.

While there is no pronounced dependence of mechanical property changes on cluster size and no variation of cluster volume fraction for weld 1, the reference RPV steel (table 5) exhibits a pronounced dependence on volume fraction compatible with the Russell–Brown model (see figure 5) and no variation of cluster size.

4. Conclusions

The SANS investigation of an RPV weld material irradiated at different levels of neutron flux (differing by a factor of 35) up to the same fluence shows that more cluster growth (by a factor of 2) occurred for the irradiation at the low flux, whereas the volume fraction of irradiation-induced clusters is essentially independent of flux. We have found that this result can be explained by the transition from a flux-independent regime of cluster growth at lower flux to a second regime, where cluster growth mediated by irradiation-enhanced Cu diffusion inversely depends on the square-root of flux. The above findings and the observed insensitivity to flux of the irradiation-induced changes of mechanical properties are inconsistent with the expectation of the dependence of yield stress on radius according to the Russell–Brown dispersion-strengthening model but are consistent with respect to the dependence on volume fraction.

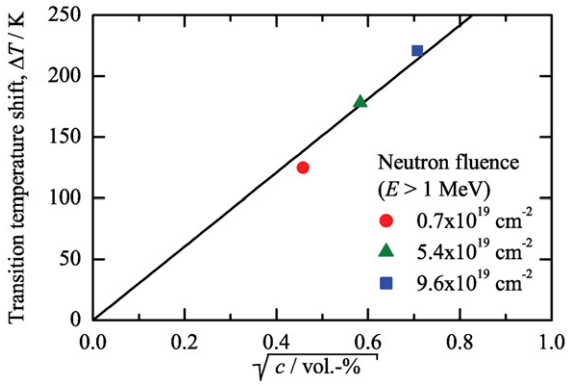

Figure 5. Correlation of the irradiation-induced shift of the brittle–ductile transition temperature and the square-root of the volume fraction of irradiation-induced clusters measured by means of SANS.

Acknowledgment

The work was funded by the German Bundesministerium für Wirtschaft (BMWi) under contract number 1501315.

References

[1] Stoller R E 2003 The effect of neutron flux on radiation-induced embrittlement in reactor pressure vessel steels *Effects of Radiation on Materials: 21st Int. Symp.* ed M L Grossbeck, T R Allen, R G Lott and A S Kumar (West Conshohocken, PA: ASTM International) pp 326–38 (ASTM STP 1447)

[2] Odette G R 1983 On the dominant mechanism of irradiation embrittlement of reactor pressure vessel steels *Scr. Metall.* **11** 1183–8

[3] Odette G R and Lucas G E 1998 Recent progress in understanding reactor pressure vessel steel embrittlement *Radiat. Eff. Defects Solids* **144** 189–231

[4] Odette G R, Wirth B D, Bacon D J and Ghoniem N M 2001 Multiscale-multiphysics modeling of radiation-damaged materials: embrittlement of pressure-vessel steels *MRS Bull.* **26** 176–81

[5] Jumel S and Van Duysen J C 2004 INCAS: an analytical model to describe displacement cascades *J. Nucl. Mater.* **328** 151–64

[6] Jumel S and Van Duysen J C 2005 RPV-1: a virtual test reactor to simulate irradiation effects in light water reactor pressure vessel steels *J. Nucl. Mater.* **340** 125–48

[7] Jumel S, Van Duysen J C, Ruste J and Domain C 2005 Interactions between dislocations and irradiation-induced

defects in light water reactor pressure vessel steels *J. Nucl. Mater.* **346** 79–97
[8] Odette G R, Yamamoto T and Klingensmith D 2005 On the effect of dose rate on irradiation hardening of RPV steels *Phil. Mag.* **85** 779–97
[9] Monasterio P R, Wirth B D and Odette G R 2007 Kinetic Monte Carlo modeling of cascade aging and damage accumulation in Fe–Cu alloys *J. Nucl. Mater.* **361** 127–40
[10] Soneda N, Ishino S, Takahashi A and Dohi K 2003 Modeling the microstructural evolution in bcc-Fe during irradiation using kinetic Monte Carlo computer simulation *J. Nucl. Mater.* **323** 169–80
[11] Odette G R 1995 *Materials Research Society Symp. Proc.* vol 373 (Warrendale, PA: Materials Research Society) p 137
[12] Odette G R 1998 *Neutron Irradiation Effects in Reactor Pressure Vessel Steels and Weldments* (Vienna: International Atomic Energy Agency) p 438 (IAEA IWG-LMNPP-98/3)
[13] Odette G R and Wirth B D 1997 A computational microscopy study of nanostructural evolution in irradiated pressure vessel steels *J. Nucl. Mater.* **251** 157–71
[14] Eason E D, Wright J E and Odette G R 1998 *Improved Embrittlement Correlations for Reactor Pressure Vessel Steels* (Washington, DC: Nuclear Regulatory Commission) NUREG/CR-6551, MCS 970501
[15] Server W L, English C A, Naiman D Q and Rosinski S T 2001 *Charpy Embrittlement Correlations—Status of Combined Mechanistic and Statistical Bases for U.S. RPV Steels* (Palo Alto, CA: Electric Power Research Institute) EPRIMRP-45 Report 1000705
[16] Debarberis L, Acosta B, Sevini F, Chernobaeva A and Kryukov A 2006 Fluence rate effect semi-mechanistic modelling on WWER-type RPV welds *J. Nucl. Mater.* **350** 89–95
[17] Ulbricht A 2006 *Thesis* TU Bergakademie Freiberg, Germany
[18] Keiderling U and Wiedenmann A 1995 New SANS Instrument at the BER II Reactor in Berlin, Germany *Physica* B **213/214** 895–7
[19] Strunz P, Saroun J, Keiderling U, Wiedenmann A and Przenioslo R 2000 General formula for determination of cross-section from measured SANS intensities *J. Appl. Crystallogr.* **33** 829–33
[20] Keiderling U 2002 The new 'BerSANS-PC' software for reduction and treatment of small angle neutron scattering data *Appl. Phys.* A **74** S1455–7
[21] Glatter O 1980 Determination of particle-size distribution functions from small angle scattering data by means of the indirect transformation method *J. Appl. Crystallogr.* **13** 7–11
[22] Solt G, Frisius F, Waeber W B and Tipping P 1993 *Effects of Radiation on Materials: 16th Int. Symp.* ed A S Kumar, D S Gelles, R K Nanstadt and E A Little (Philadelphia, PA: ASTM) p 444 (ASTM STP 1175)
[23] Mathon M H, Barbu A, Dunstetter F, Maury F, Lorenzelli N and De Novion C H 1997 Experimental study and modelling of copper precipitation under electron irradiation in dilute FeCu binary alloys *J. Nucl. Mater.* **245** 224–37
[24] Miller M K, Russell K F, Sokolov M A and Nanstad R K 2005 Atom probe tomography of radiation-sensitive KS-01 weld *Phil. Mag.* **85** 401–8
[25] Pareige P, Radiguet B, Krummeich-Brangier R, Barbu A, Zabusov O and Kozodaev M 2005 Atomic-level observation with three-dimensional atom probe of the solute behaviour in neutron-, ion- or electron-irradiated ferritic alloys *Phil. Mag.* **85** 429–41
[26] Mansur L K 1978 Void swelling in metals and alloys under irradiation: an assessment of the theory *Nucl. Technol.* **40** 5–34
[27] Ulbricht A and Böhmert J 2004 Small angle neutron scattering analysis of the radiation susceptibility of reactor pressure vessel steels *Physica* B **350** e483–6
[28] Ulbricht A, Böhmert J and Viehrig H W 2005 Microstructural and mechanical characterization of radiation effects in model reactor pressure vessel steels *J. ASTM Int.* **10** JAI12385
[29] Ulbricht A, Bergner F, Dewhurst C D and Heinemann A 2006 Small-angle neutron scattering study of post-irradiation annealed neutron irradiated pressure vessel steels *J. Nucl. Mater.* **353** 27–34
[30] Russell K C and Brown L M 1972 A dispersion strengthening model based on differing elastic moduli applied to the iron–copper system *Acta Metall.* **20** 969–74
[31] Nedelcu S, Kizler P, Schmauder S and Moldovan N 2000 Atomic scale modeling of edge dislocation movement in the α-Fe–Cu system *Modelling Simul. Mater. Sci. Eng.* **8** 181–91